Article

Cell Host & Microbe

Apical Invasion of Intestinal Epithelial Cells by *Salmonella typhimurium* Requires Villin to Remodel the Brush Border Actin Cytoskeleton

Graphical Abstract

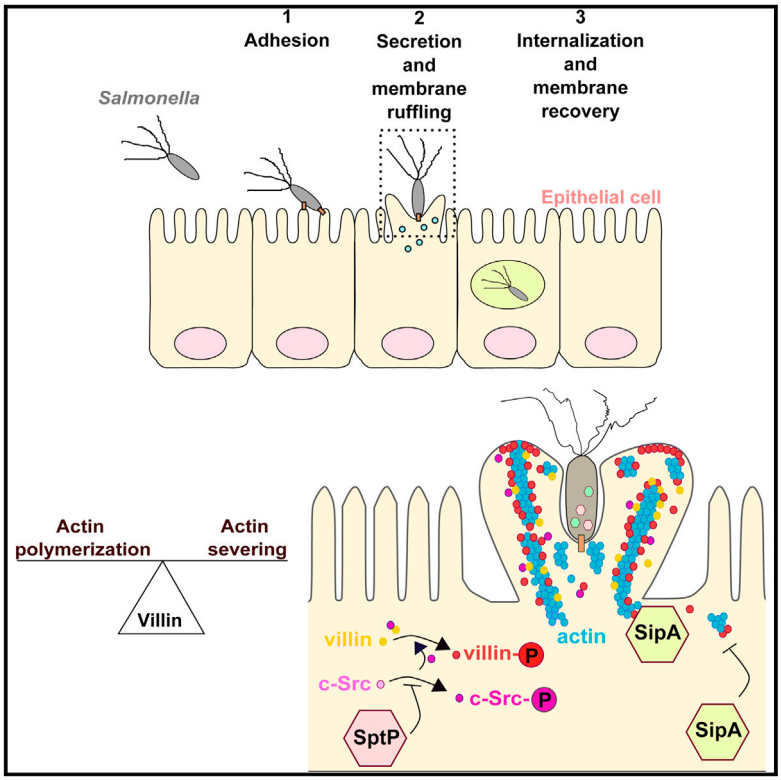

Highlights

- The host actin-binding protein villin is required for *Salmonella* apical invasion
- Villin plays a role in *Salmonella* ruffle formation and actin dynamics
- Villin-severing activity promotes *Salmonella* invasion in cells and in vivo
- The bacterial effectors SipA and SptP regulate villin activities

Authors

Nouara Lhocine, Ellen T. Arena, ..., Sylvie Robine, Philippe J. Sansonetti

Correspondence

philippe.sansonetti@pasteur.fr

In Brief

Salmonella interacts directly with the brush border of intestinal epithelial cells to promote its internalization. Lhocine et al. demonstrate that the rapid cytoskeleton remodeling at the bacterial entry site requires villin, an apical actin-binding protein. Villin is the target of bacterial effectors, SipA and SptP, which regulate its actin-modifying properties.

Lhocine et al., 2015, Cell Host & Microbe *17*, 164–177
February 11, 2015
http://dx.doi.org/10.1016/j.chom.2014.12.003

CellPress

Cell Host & Microbe
Article

Apical Invasion of Intestinal Epithelial Cells by *Salmonella typhimurium* Requires Villin to Remodel the Brush Border Actin Cytoskeleton

Nouara Lhocine,[1,2] Ellen T. Arena,[1,2] Perrine Bomme,[4] Florent Ubelmann,[5,6] Marie-Christine Prévost,[4] Sylvie Robine,[5] and Philippe J. Sansonetti[1,2,3,*]
[1]Unité de Pathogénie Microbienne Moléculaire
[2]INSERM U786
Institut Pasteur, 25 rue du Docteur Roux, 75015 Paris, France
[3]Collège de France, 11 Place Marcelin Berthelot, 75005 Paris, France
[4]Plateforme de Microscopie Ultrastructurale, Institut Pasteur, 25 rue du Docteur Roux, 75015 Paris, France
[5]Unité Mixte de Recherche 144, Institut Curie, 75248 Paris Cedex 05, France
[6]Centro de Estudos de Doenças Crónicas (CEDOC), Faculdade de Ciencias Médicas, Universidade Nova de Lisboa, 1169-056, Portugal
*Correspondence: philippe.sansonetti@pasteur.fr
http://dx.doi.org/10.1016/j.chom.2014.12.003

SUMMARY

Salmonella **invasion of intestinal epithelial cells requires extensive, though transient, actin modifications at the site of bacterial entry. The actin-modifying protein villin is present in the brush border where it participates in the constitution of microvilli and in epithelial restitution after damage through its actin-severing activity. We investigated a possible role for villin in *Salmonella* invasion. The absence of villin, which is normally located at the bacterial entry site, leads to a decrease in *Salmonella* invasion. Villin is necessary for early membrane-associated processes and for optimal ruffle assembly by balancing the steady-state level of actin. The severing activity of villin is important for *Salmonella* invasion in vivo. The bacterial phosphatase SptP tightly regulates villin phosphorylation, while the actin-binding effector SipA protects F-actin and counterbalances villin-severing activity. Thus, villin plays an important role in establishing the balance between actin polymerization and actin severing to facilitate the initial steps of *Salmonella* entry.**

INTRODUCTION

Salmonella enterica serovar *typhimurium* (*S. typhimurium*) is a facultative intracellular pathogen that has developed powerful strategies to infect the gastrointestinal tract. This bacteria uses various routes to invade the gut epithelial barrier: penetration through intestinal epithelial cells (IECs), invasion of Peyer's patches via M cells, and paracellular access to the *lamina propria* by breaching tight junctions or following capture by dendritic cells (Watson and Holden, 2010). *Salmonella* is able to interact directly with the brush border of IECs to promote internalization (Finlay and Falkow, 1990). Microbial invasion of IECs requires extensive, though transient, host cytoskeleton modifications at the bacterial entry site, leading to dramatic changes in the architecture of the brush border. Actin rearrangements play a central role in this process of bacterial uptake (Ly and Casanova, 2007). Rapid actin polymerization is observed at the bacterial entry site. However, rapid subsequent cytoskeleton disassembly is necessary to return the membrane structure to normal. Fast actin depolymerization is critical for actin-dependent processes, but it is not clear whether this is a crucial point during bacterial invasion.

An array of bacterial factors enables interaction with and active invasion of the intestinal epithelium through IECs (Agbor and McCormick, 2011). A type-three secretion system is used to inject these effector proteins into the cytosol of host cells in order to induce rapid actin polymerization and membrane ruffling (Ly and Casanova, 2007). The bacterial actin-binding proteins (ABPs) SipA and SipC promote the formation of actin filaments at the bacterial entry site and prevent filament disassembly by host factors, such as the ABPs gelsolin and cofilin (Hayward and Koronakis, 1999; Zhou et al., 1999a, 1999b). SopE/SopE2 and SopB activate Rho-GTPases, such as Rac1 and Cdc42, to favor the constitution of a highly branched actin network (Hardt et al., 1998; Hong and Miller, 1998; Steele-Mortimer et al., 2000; Stender et al., 2000; Zhou et al., 2001). After internalization, the actin cytoskeleton returns to its steady state through the inactivation of Rac and Cdc42 by the bacterial GTPase-activating protein SptP (Fu and Galán, 1999). This effector is also a tyrosine phosphatase that re-establishes host cell integrity by inhibiting the phosphorylation of host proteins, such as vimentin (Murli et al., 2001). Therefore, both actin polymerization and depolymerization need to occur simultaneously to enable actin filaments formation and relocation.

During development, IECs differentiate into tightly adherent polarized cells that form a physical and physiological barrier, protecting the host from infection. At their apical surface, these cells present microvilli that increase the cell surface area and favor absorptive and secretory functions. These microvilli consist of uniformly polarized cross-linked actin filaments. Their modifications depend on ABPs that can polymerize, bundle,

depolymerize, sever, or cap actin filaments. Among these ABPs, villin is an abundant epithelial actin-modifying protein present in the brush border and responsible for the establishment of the structure and function of the microvilli (Revenu et al., 2012). Villin participates in the constitution of epithelial cell structures by regulating actin dynamics. Indeed, villin itself can cap, sever, nucleate, or bundle actin filaments (Khurana and George, 2008). Villin activities are regulated not only by posttranslational modifications, including tyrosine phosphorylation (Tomar et al., 2004), but also by phosphatidylinositol 4,5-bisphosphate (PIP2) or lyso-phosphatidic acid (LPA) (Khurana and George, 2008). These molecules control villin properties and allow it to switch among its different functions. Moreover, actin binding by villin depends on intracellular calcium concentrations (Bretscher and Weber, 1980; Kumar et al., 2004a; Kumar and Khurana, 2004). At high calcium concentrations, the severing function of villin is activated. However, severing can also be established when calcium concentrations are low if villin is phosphorylated, inducing a decrease in the pool of F-actin. The ligand-binding properties of villin are mechanistically important for the crosstalk between signaling cascades and actin remodeling in IECs, suggesting villin is also an important regulatory target.

It has been demonstrated in vivo that villin knockout mice display a normal brush border with functional microvilli, indicating that other proteins may have similar functions on actin organization. However, during stress conditions that modify calcium concentrations, such as DSS treatment, the lack of villin impacts cell reorganization and plasticity (Ferrary et al., 1999). These results suggest that villin plays an important role in actin dynamics in response to physiological or pathological stimuli. It has been shown that villin is recruited at the interaction site with the parasites *Cryptosporidium parvum* (Forney et al., 1999) and *Entamoeba histolytica* (Lauwaet et al., 2003), and at the entry site of *Listeria monocytogenes* (Temm-Grove et al., 1994). Moreover, this protein is required in vivo for *Shigella flexneri* infection, as villin knockout mice are resistant to gut invasion by *Shigella* (Athman et al., 2005; Fernandez et al., 2003). In particular, it has been shown that villin-severing activity is necessary for *Shigella* motility inside host cells (Revenu et al., 2007). However, the actual involvement of this activity in pathogenic adhesion and invasion is not known. *Shigella* invades the intestinal epithelium through M cells or by opening paracellular junctions, contrary to *Salmonella*, which interacts directly with the brush border of the IECs. *Salmonella* is therefore a more appropriate model to study the involvement of villin in bacterial invasion.

Here we investigated a possible role for villin in *Salmonella* invasion of the intestinal epithelium. We examined the effects of the downregulation of *villin* expression during *Salmonella* infection in TC7 cells. Using a streptomycin mouse model of enterocolitis (Hapfelmeier and Hardt, 2005), we also analyzed the impact of villin on *Salmonella* invasion in vivo. Through a combination of in vitro and in vivo approaches, our data indicate that the absence of villin, which is normally located at the entry site of *Salmonella*, leads to a decrease in apical invasion of IECs, reflected in reduced inflammation and mucosal destruction in the infected intestinal mucosa. Dedicated type-III bacterial secreted effectors account for the modulation of villin activities through phosphorylation, particularly its severing activity. Our results therefore demonstrate an important role for villin during the initial steps of apical entry of *Salmonella*.

RESULTS

Villin Is Recruited to *Salmonella*-Induced Ruffles

Upon reaching the membrane, *Salmonella* induce cytoskeleton rearrangements to assemble specific actin-rich structures called ruffles, which are associated with the entry sites of the bacteria. We explored the role that villin may play in membrane ruffling of polarized IECs. As villin is expressed and properly distributed only in differentiated IECs, we used a cellular model that enables an endogenous apical expression of this protein after differentiation (i.e., human colonic TC7 cells). This cell line can differentiate into polarized cells with a functional brush border. In differentiated cells, villin was located at the apex of the cells and colocalized with the actin cytoskeleton in the microvilli (Figure 1A). Within *Salmonella*-infected cells, when ruffles were formed, villin concentrated mainly around the bacterial bodies in association with actin (Figures 1B and 1C). However, villin did not colocalize with *Salmonella*-containing vacuoles inside the host cytoplasm (data not shown). Confocal microscopy revealed the existence of an upper layer of villin not associated with actin, though seeming to form the ruffle (Figure 1D). In a second layer, actin and villin colocalized. Finally, deep inside the ruffle, villin-free actin was observed. This organized distribution suggests that villin could play a key role in leading ruffle assembly during initial *Salmonella* invasion.

Villin Promotes the Invasion of IECs by *Salmonella*

To gain further insight into the functional significance of villin during *Salmonella* infection, *villin* expression was silenced through stable transduction with recombinant lentiviruses expressing shRNAs targeting two independent sites in the *villin* mRNA (i.e., sh-vil1 and sh-vil2). A nonsilencing shRNA was used as a control (sh-scr). Western blots of stably transduced TC7 cells were performed after differentiation and showed a decrease in villin production (Figure S1A available online). These data confirmed RT-qPCR experiments (Figure S1B). Immunofluorescence was performed to study the morphology of villin knockdown cells (Figure 2A). Actin staining was not modified, having a strong apical and lateral signal. Cells did not exhibit any morphological defect. Microvilli were terminally differentiated as observed by scanning electron microscopy (SEM) (Figure 2D, panel D).

To study the effects of villin knockdown on bacterial entry, control and villin knockdown cells were infected with *S. typhimurium*, and invasion was measured by gentamicin assays (Figure 2B). The noninvasive *prgh* mutant was used as a control. A significant decrease in the number of CFU was observed 1 hr postinfection (p.i.) in villin knockdown cells compared to control cells. Indeed, *Salmonella* invasion was reduced by 44% with sh-vil1 ($p < 0.01$) and 49% with sh-vil2 ($p < 0.001$). As the two *villin*-specific shRNAs had comparable effects in all assays, only the data obtained with sh-vil1 are presented. To confirm previous results, the number of intracellular bacteria per cell was determined by confocal microscopy following washing and bacterial staining (Figure 2C). Villin knockdown was associated with a significant decrease in the number of internalized bacteria ($p < 0.001$).

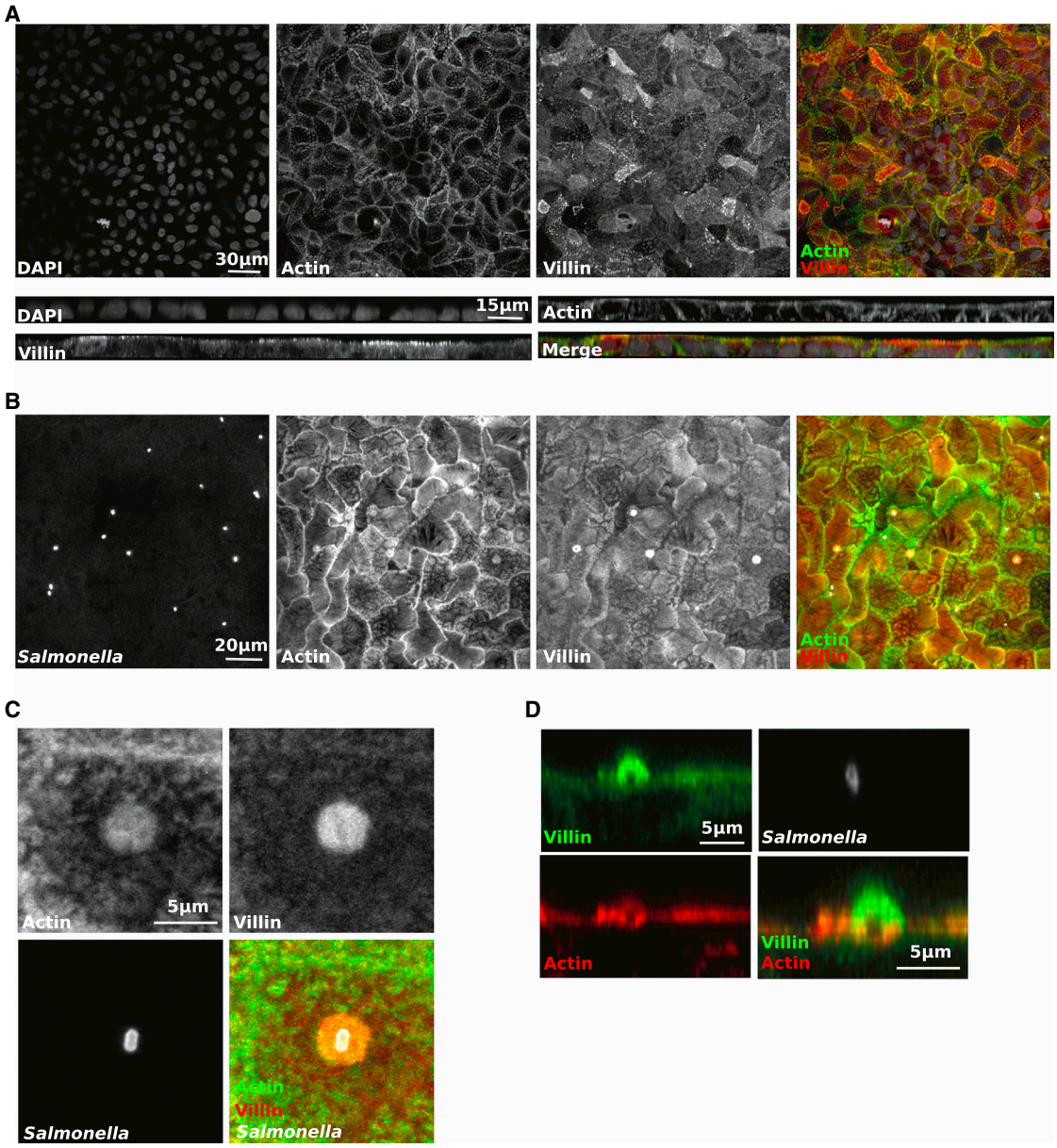

Figure 1. Villin Is Recruited at the Entry Site of *Salmonella*

(A–D) (A) Uninfected polarized TC7 or (B) infected with *S. typhimurium* for 15 min (MOI20) were fixed and stained with an anti-villin antibody and FITC-phalloidin to label F-actin. Bacteria were labeled with an anti-LPS antibody, and nuclei were counterstained with DAPI. Cells were visualized under a confocal microscope. Top view ([A] and [B]) and side view (A) are represented. Zoom from a top view (C) and a side view (D) of a *Salmonella*-induced ruffle.

Villin Participates in the Formation of *Salmonella*-Induced Ruffles

To further explore the role of villin during *Salmonella* invasion, SEM was used to assess the consequence of villin level reduction on ruffle formation. As shown in Figure 2D (panels B and C), sh-scr cells supported the formation of ruffles with a characteristic doughnut-like structure. These ruffles displayed a particular radial symmetry and were formed mainly around single bacteria. In contrast, in sh-vil1 cells, a major modification in ruffle morphology was observed (Figure 2D, panels E and F). They lost their normal, symmetrical structure and appeared disorganized, with many aberrant protrusions and an apparent defect in the fusion of membrane extensions. These ruffles were diffused and often associated with multiple bacteria.

Villin Participates in the Reorganization of the Actin Cytoskeleton

Salmonella invasion is dependent upon actin polymerization to generate the forces required to invade IECs. The recruitment of host-cell proteins to *Salmonella*-induced ruffles was therefore examined by immunofluorescence. Although villin-knockdown notably decreased *Salmonella* invasion, this did not lead to a

defect in actin recruitment per se, as we could still observe actin at the entry site of *Salmonella* (Figure 3A). However, confocal microscopy revealed that this actin recruitment showed a broader base at the entry site and did spread much more extensively in sh-vil1 cells.

To decipher if villin knockdown could produce effects on the actin cytoskeleton, we quantified the impact on actin polymerization during *Salmonella* invasion. Cells were infected, and staining of fixed cells was performed with phalloidin to visualize the F-actin content in the invasion ruffles. Only ruffles containing one single bacterium were taken into account to avoid any potential artifacts. Using Imaris software, the diameter and the volume of 100 invasion sites were measured (Figure 3B). We observed radial symmetric recruitment of actin in the ruffles with an average diameter of 3.396 μm and a range of 2.12–4.94 μm in sh-scr cells. In contrast, ruffles in sh-vil1 cells exhibited a more diffuse staining, with an average diameter of 4.065 μm and a range of 2.57–9.08 μm. The knockdown of villin induced an increase of the F-actin content in the invasion ruffles compared to sh-scr cells (Figure 3B). The actin volume content in the ruffles was significantly higher in the absence of villin, with a range of 7.410–103 μm^3 in control cells and 16.3–126 μm^3 in sh-vil1 cells. Consequently, villin influences actin remodeling at the entry sites and is therefore required for regulation of the early membrane-associated processes.

To confirm that villin has a role in modulating actin dynamics during *Salmonella* infection, we assayed F- and G-actin contents. After separation by ultracentrifugation, F- and G-actin contents were measured via western blot and quantified by densitometric scanning (Figure 3C). In sh-scr cells, the F-actin content was constant during the course of the infection, in agreement with published data (Higashide et al., 2002). This indicates that the total cellular quantity of F-actin is controlled during *Salmonella* infection, even though massive amounts of F-actin accumulate at the entry site of the bacteria. In uninfected sh-vil1 cells, a decrease in the F-content was observed with a reorganization of the F-actin, whereas the G-actin content was not affected. This is consistent with previously published data (Friederich et al., 1989; Wang et al., 2012). Thus, although sh-vil1 cells did not exhibit abnormal morphologies, the F-actin content of the cells was perturbed. Interestingly, *Salmonella* infection leads to a significant increase in the amount of F-actin but not G-actin. There is a strong imbalance of the F-actin ratio in the absence of villin, indicating that this protein is essential to equilibrating F-actin content during invasion. Therefore, these results demonstrate that villin plays an important role in maintaining the steady-state level of F-actin during *Salmonella* infection.

The Bacterial Effector SipA Regulates Villin Activities

We tested the effect of villin downregulation on *Salmonella* invasion in the absence of bacterial effectors known to regulate the actin cytoskeleton (Figure 4A). In sh-scr cells, the absence of *SipA*, *SipC*, *SptP*, or *SopE/SopE2/SopB/SipA* leads to a significant decrease in *Salmonella* invasion. In sh-vil1 cells, the inactivation of *SipC* or *SopE/SopE2/SopB/SipA* leads to a stronger decrease in the invasion compared to control cells, whereas *SipA* or *SptP* did not induce such a decrease, indicating that these two proteins could be putative regulators of villin activities.

SipA is an ABP that inhibits actin turnover by displacing host ABPs from F-actin. This effector protects F-actin from severing, therefore enabling its polymerization (Zhou et al., 1999b; McGhie et al., 2001, 2004). SipA colocalized with villin at the bacterial entry site (Figure 4B). *Salmonella* mutants lacking *SipA* entered less efficiently into control cells. In agreement with published results, numerous ruffles were observed on sh-scr cells (Figure 4C, middle panel). The *SipA* mutant induced the formation of projections that contain actin at the base of the ruffle, but mainly villin in the apical part (Figure 4C, middle panel), exacerbating what was observed with wild-type (WT) *Salmonella* (Figure 4C, upper panel). These projections were asymmetrical and highly extended at late time points (Figure 4C, lower panel). These observations indicate that the first steps in induction of membrane ruffling are not affected by the loss of *sipA.* As SipA counteracts the severing activity of ADF and cofilin, we tested whether or not it would be the case with villin. To investigate a potential interplay between SipA and villin, in vitro assays of actin dynamics were performed (Figure 4D). Villin protein (Vill) or a mutated form for the severing activity domain (VillΔSev) were purified and added to Rh-labeled F-actin. The polymerization state of F-actin was visualized directly by fluorescence microscopy. Whereas the WT protein induced actin severing, the mutated form did not modify F-actin structure. The addition of SipA alone did not lead to any change in actin polymerization. In contrast, when SipA was added simultaneously with the WT villin, actin severing induced by villin was inhibited. These results suggest that SipA protects F-actin from villin-directed severing.

Previous studies have shown that the C-terminal region of SipA contains a functional domain responsible for its actin-modulating activity (amino acids 460 to 685) and that the minimal region to promote this activity is $SipA_{514\text{-}657}$. Moreover, it has been described that the amino acid residues K635 and E637 are necessary for G-actin polymerization (Li et al., 2013). We first decided to test if this minimal domain could be sufficient to inhibit villin-severing activities. We observed that similarly to SipA, $SipA_{514\text{-}657}$ counteracted the severing activity of villin (Figure 4D), contrary to the shorter isoform $SipA_{514\text{-}640}$ that does not retain this activity. The $SipA_{514\text{-}657}^{K635AE637W}$ isoform that is not able to polymerize G-actin has also lost the ability to block villin functions, indicating that the capacity of SipA to polymerize G-actin is necessary to counterbalance villin-severing activities.

SptP Tightly Regulates Villin Phosphorylation during *Salmonella* Infection

The identification of villin as a putative target for the tyrosine phosphatase SptP prompted us to examine potential villin targeting by this bacterial effector. First, SptP localization during infection was studied (Figure 5A). This protein colocalized with villin in the ruffles. Interestingly, the site of invasion is a region of intensive phosphorylation activity (Figure 5B). Therefore, we tested the effect of the phosphatase SptP on villin phosphorylation. Cells were infected with WT *S. typhimurium* or its isogenic *SptP* mutant, and villin phosphorylation was examined during the course of infection. Tyrosine phosphorylated proteins were immunoprecipitated, and villin was detected by western blotting (Figure 5C). An increase in villin phosphorylation was observed 15 min p.i. with the WT strain, followed by a decrease 30 min p.i. In the absence of the bacterial phosphatase SptP, villin

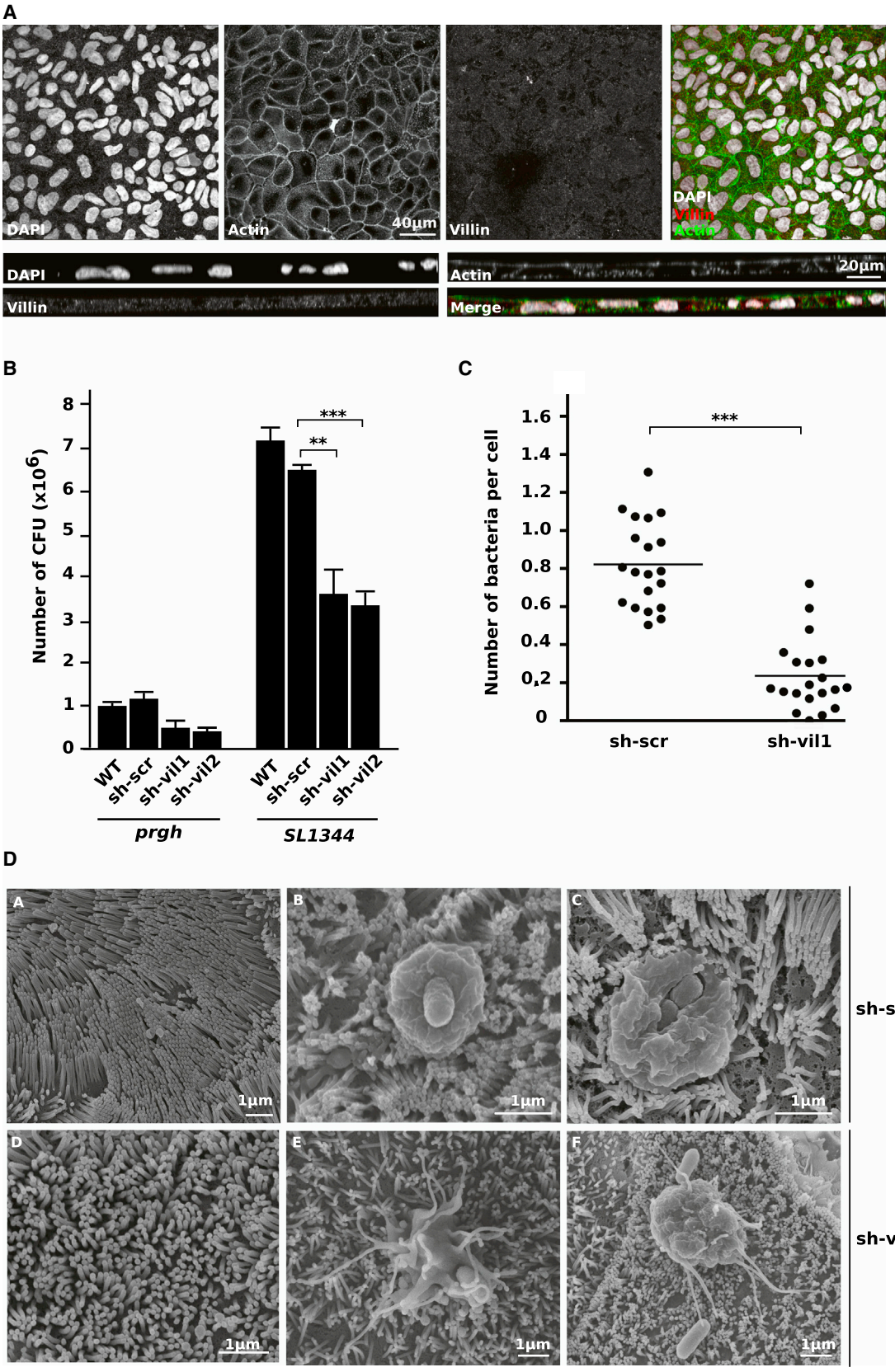

(legend on next page)

phosphorylation was observed earlier during the course of infection, indicating that SptP prevents villin phosphorylation at the beginning of the invasion process.

To ensure that SptP phosphatase activity is responsible for this increase, cells were infected with a strain expressing a phosphatase-inactive full-length mutant of SptP ($SptP^{C481S}$) (Figure 5C). In this context, villin phosphorylation was also modified with a strong increase observed within 5 min p.i., confirming that the phosphatase activity of SptP inhibits villin phosphorylation during the first steps of infection. As tyrosine phosphorylation of villin can modify its binding activity to F-actin in vitro, as well as its actin nucleation and severing activities (Zhai et al., 2001), we therefore tested if villin phosphorylation in infected cells modified its binding to actin. We took advantage of the *SptP* mutant that exhibits a significant increase in villin phosphorylation early during the invasion process. A coimmunoprecipitation experiment was performed to detect potential modifications in actin binding to villin during the course of infection. As shown in Figure 5D, with the *SptP* mutant, we could detect an increase in actin coimmunoprecipitated with villin, indicating that villin phosphorylation affects its actin binding capacities.

c-Src Is Responsible for Villin Phosphorylation during *Salmonella* Infection

The tyrosine kinase c-Src regulates the phosphorylation of villin in vitro and in cells under physiological conditions (Mathew et al., 2008). c-Src activities are also regulated through phosphorylation. Indeed Y416 is a major phosphorylation site necessary for c-Src activation. Interestingly, c-Src phosphorylation occurred during *Salmonella* infection (Figure 5D) and appeared even more important in the absence of the phosphatase SptP, indicating that this bacterial effector regulates c-Src activities. To test if this kinase could be responsible for villin phosphorylation during *Salmonella* infection, their interaction was first tested by coimmunoprecipitation. Villin was immunoprecipitated and c-Src coimmunoprecipitation was visualized by western blot (Figure 5E). As expected, c-Src is coimmunoprecipitated under noninfectious conditions. We observed an increase in this coimmunoprecipitation 15 min p.i. with *Salmonella*. To confirm that c-Src is responsible for villin phosphorylation upon infection, the activity of this kinase was inhibited with PP2, an inhibitor for Src-family kinases that downregulates pSrc-416 (Figure 5F). Whereas a strong increase in villin phosphorylation was observed in the absence of PP2 when cells were infected with SptP, this was not observed when c-Src was inactivated with the drug (Figure 5G). These results indicate altogether that this kinase is responsible for villin phosphorylation during *Salmonella* infection, but also SptP controls villin phosphorylation by c-Src through pSrc-416 regulation.

Villin-Deficient Mice Exhibit Attenuated Intestinal Pathology

To assess the function of villin during host infection by *S. typhimurium*, age- and sex-matched $Villin^{+/+}$ ($Vil^{+/+}$) and $Villin^{-/-}$ ($Vil^{-/-}$) mice were orally infected with *S. typhimurium*. Villin knockout mice are viable, fertile and have normal lifespans (Ferrary et al., 1999). Histological changes were evaluated in infected mice on intestinal sections that were H&E stained. Infection of $Vil^{+/+}$ mice with *S. typhimurium* resulted in severe enteritis with typical hallmarks of inflammation, including pronounced edema in the submucosa, disruption of the crypt architecture, loss of goblet cells, epithelial erosion, and infiltration of polymorphonuclear neutrophils (Figure 6A). Already at 24 hr p.i., $Vil^{+/+}$ mice exhibited pathological changes that were more severe compared to $Vil^{-/-}$ mice. These histological differences were even more striking at 48 and 72 hr. The epithelial lining from $Vil^{+/+}$ mice was more destroyed with diffused desquamation; the lumen was filled with dead epithelial cells and the sub-mucosa was oedematous. In contrast, intestines from $Vil^{-/-}$ mice were much less inflamed with attenuated destruction. To determine if these effects were due to a differential colonization of the intestinal tissues by the bacteria, the bacterial load of *Salmonella* in the small intestine was determined at 24 hr. At day1 p.i., $Vil^{-/-}$ mice did not exhibit a reduced bacterial load in the intestine (Figure 6B).

To better characterize any effect on luminal colonization or the intestinal tissue, immunofluorescence staining was performed on tissue sections to precisely determine the location of bacteria (Figure 6C). The intestinal lumen of $Vil^{-/-}$ mice was heavily colonized by bacteria, with little tissue invasion, in contrast with $Vil^{+/+}$ mice that had pronounced bacterial invasion of the mucosal tissue. These results clearly indicate that *S. typhimurium* invades intestinal tissues of $Vil^{+/+}$ mice more efficiently. Finally, invasion of the intestinal mucosa by *Salmonella* was linked to an early acute proinflammatory response. In $Vil^{-/-}$, the reduced histological changes correlated with a decreased expression of proinflammatory cytokine genes, such as *IL-6* and *IL-1β*, as assessed by RT-qPCR at 24 and 48 hr p.i. (Figure 6D). Consequently, animals lacking villin show a delayed inflammatory response.

Mice Mutated for the Severing Domain of Villin Are More Resistant to *Salmonella* Infection

Several clues tend to indicate that actin-severing activities could play an important role during *Salmonella* infection. First, actin

Figure 2. *Villin* Silencing Leads to a Decrease in Apical *Salmonella* Invasion

(A) Villin and F-actin distribution in uninfected polarized sh-vil1 TC7. Nuclei were counterstained with DAPI. Upper part: top view of the cells; lower part: side view. (See also Figure S1.)

(B) Gentamicin assays. WT, sh-scr, sh-vil1, and sh-vil2 cells were infected for 1 hr with noninvasive (*prgh*) or WT (*SL1344*) *Salmonella* (MOI 100), treated for 1 hr with gentamicin, lysed with 1% triton, and plated to count intracellular CFU. Data are represented as mean ± SEM (***$p < 0.001$; **$p < 0.01$, Mann-Whitney).

(C) Invasion assays performed by bacterial immunolocalization. Intracellular and extracellular bacteria were stained with an anti-LPS antibody before and after cell permeabilization of sh-scr and sh-vil1 cells infected with *Salmonella* for 1 hr (MOI 10). Bacterial invasion was quantified by inside/outside differential staining. The average number of bacteria per cell was counted in 20 different fields by fluorescence microscopy (Imaris software). Each point represents data obtained from one field. Data are represented as mean ± SEM (***$p < 0.001$).

(D) *Salmonella*-induced ruffles are perturbed in absence of villin in polarized IECs. Representative SEM micrographs of sh-scr ([D_A]–[D_C]) or sh-vil1 ([D_D]–[D_F]) monolayers not infected ([D_A] and [D_D]) or infected with *S. typhimurium* ([D_B], [D_C], [D_E], and [D_F]) for 30 min (MOI 20).

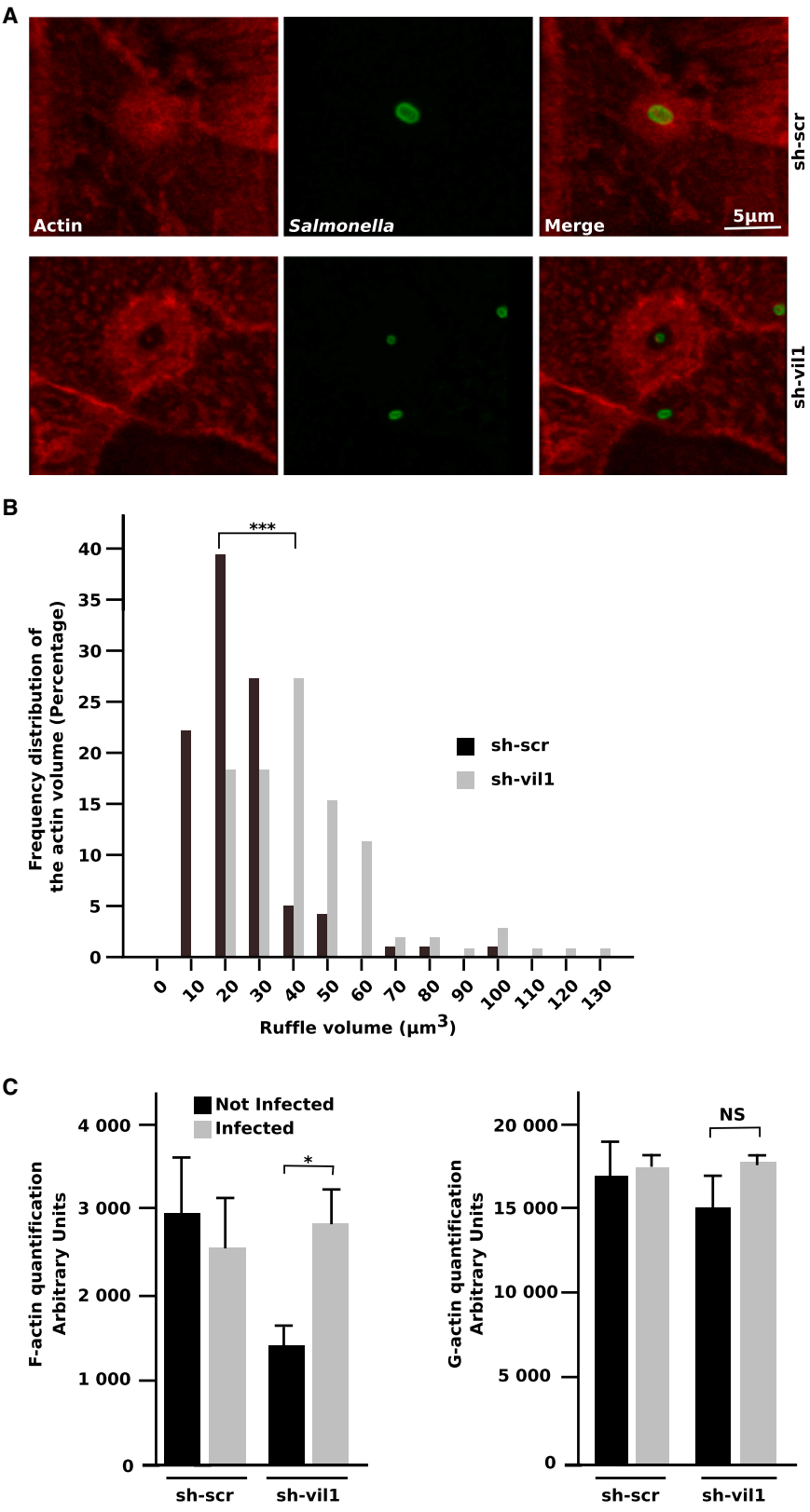

Figure 3. *Villin* Silencing Perturbs the F-Actin Content upon *Salmonella* Invasion

(A) Immunolocalization of bacteria (anti-LPS antibody, green) in sh-scr (upper panel) and sh-vil1 (lower panel) cells (MOI20). F-actin is labeled with Alexa647-phalloidin (red).

(B) Actin volume distribution in ruffles from sh-scr (black bars) and sh-vil1 (gray bars) cells 1 hr p.i. (MOI10). Actin volume was quantified with the Imaris software (***$p < 0.001$, Mann-Whitney).

(C) F- and G-actin quantification in sh-scr and sh-vil1 cells (MOI100). The F-actin content was separated from the G-actin content by ultracentrifugation and quantified by densitometric measure on western blots. Black bars represent uninfected cells, and gray bars represent *Salmonella*-infected cells. Data are represented as mean ± SEM (*$p < 0.05$; NS, not significant; Unpaired t test with Welch's Correction).

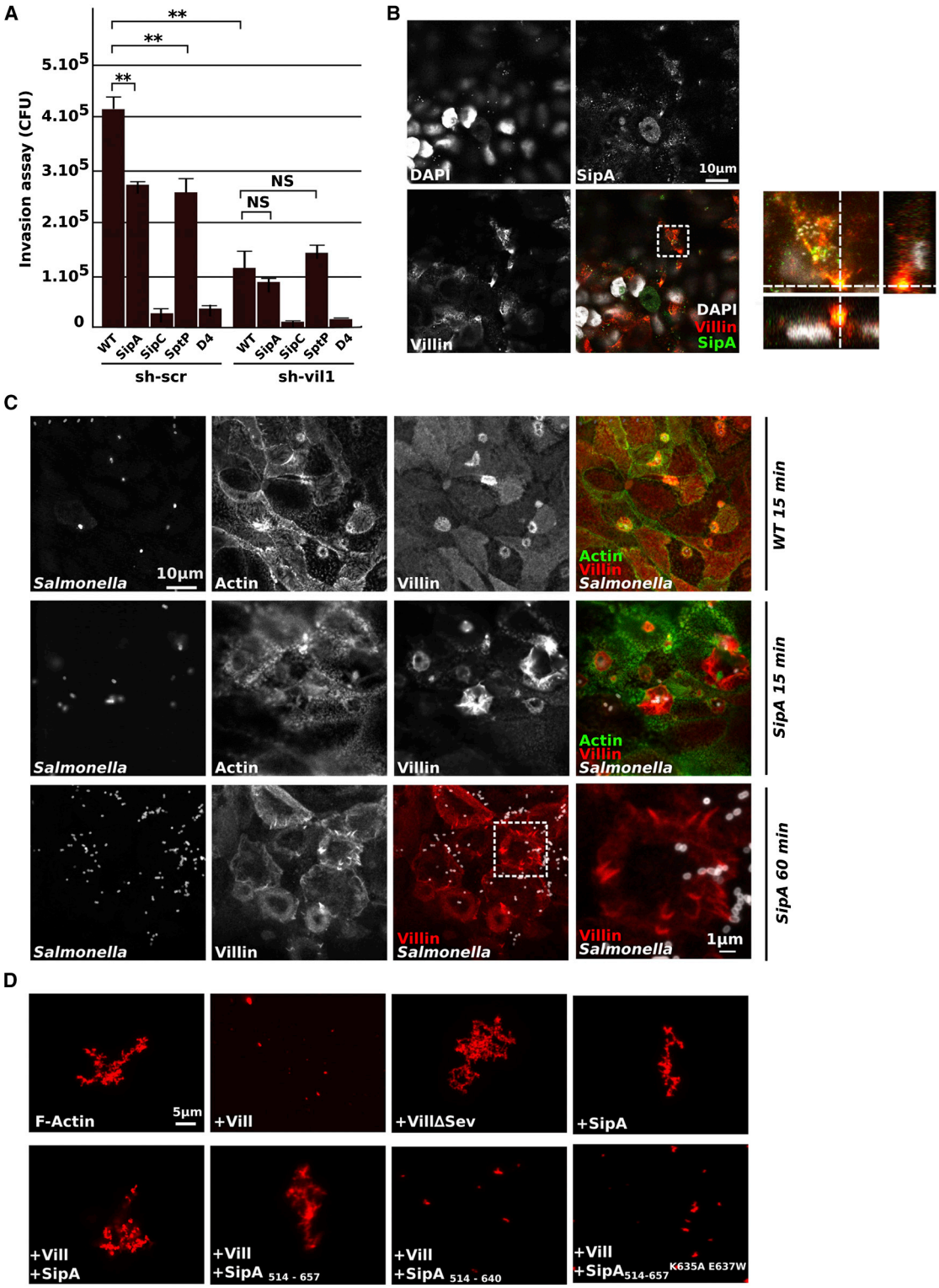

Figure 4. The Bacterial Effector SipA Inhibits Villin-Severing Activities

(A) Gentamicin assays. sh-scr and sh-vil1 cells were infected for 1 hr with WT (*SL1344*) or mutated (*SipA*; *SipC*; *SptP*; or D4 for *SopE*, *SopE2*, *SopB*, *SipA*) *Salmonella* (MOI100), treated for 1 hr with gentamicin, lysed with 1% triton, and plated to count intracellular CFU. Data are represented as mean ± SEM (**$p < 0.01$; NS, not significant; Unpaired t test).

(B) Villin (red) and SipA (green) distribution in sh-scr cells infected with *Salmonella* for 1 hr. In the right panel a magnification of the squared area with X-Z and Y-Z cross-sections.

(legend continued on next page)

polymerization occurs despite the absence of villin. Second, the two identified bacterial regulators seem to control severing events. Moreover, villin-severing activity is essential for the apical remodeling during epithelial restitution after damage (Ubelmann et al., 2013). Therefore, we decided to test the importance of villin-severing activity in vivo during the first steps of *Salmonella* invasion. We used transgenic mice that are knockout for *villin* but re-express a wild-type (*tgvillinWT*) or a severing mutated form (*tgvillinΔsev*) in the intestinal cells after induction with tamoxifen (Ubelmann et al., 2013). These mice were infected with *Salmonella* for 24 hr. Histological changes were evaluated in infected mice. After infection, *tgvillinWT* mice exhibited significant pathological changes compared to *tgvillinΔsev* mice at the level of the epithelial lining (Figure 7A). Immunofluorescence staining performed on small intestine samples indicated that *Salmonella* can be found in close contact with the epithelium in both cases, but intracellular bacteria were only found in *tgvillinWT* (Figure 7B). Finally, intestinal mucosa invasion by *Salmonella* was linked to an early acute proinflammatory response in the presence of villin WT in the epithelial cells (Figure 7C). Indeed, *tgvillinΔsev* mice showed a delayed inflammatory response. Therefore, the animals lacking the severing activity of villin in the intestinal epithelium are more resistant to *Salmonella* infection.

DISCUSSION

Considering the complex and highly organized cytoskeletal structure of the apical brush border, one expects that its subversion precedes and participates with bacterial invasion of polarized IECs by pathogens, including *Salmonella*. Taking into account its developmental and functional characteristics, villin was an obvious target candidate for a pathogen's subversion of the brush border. Our results demonstrate that villin is required for apical invasion of IECs by *Salmonella* and necessary for early membrane-associated processes and for optimal ruffle assembly by balancing the steady-state level of actin. Villin-severing activities can promote brush border dissociation and microvilli remodeling upon *Salmonella* adhesion, leading to a better engagement of the membrane by the bacteria. This is in agreement with published data indicating that treatment with cytochalasin D disrupts actin and unexpectedly leads to an increase in *Salmonella* invasion of polarized Caco-2 and HT-29 cells, but not of HeLa cells (Wells et al., 1998).

Membrane ruffling is due to intense polymerization events that produce strong mechanical actin-based forces. However, these forces have to be constrained and highly driven to promote efficient and targeted invasion. The F-actin content is not modified during *Salmonella* invasion, suggesting that a tight control exists to balance between simultaneous actin polymerization and depolymerization activities that relax the mechanical pressure induced by the ruffle and to allow directional protrusions (Higashide et al., 2002). Interestingly, when microvilli differentiate, actin polymerization appears sufficient to create a force that overcomes resistance of the apical membrane to bending (Mogilner and Rubinstein, 2005). Therefore the length of the microvilli may largely depend on the length and rigidity of actin filaments, and therefore on actin polymerization capacities. It has been previously shown that *Salmonella* invasion is more efficient in polarized cells than in nonpolarized cells (Lorkowski et al., 2014), and according to our results, this could be explained by villin. Indeed, polymerization activities are supported by several bacterial factors during *Salmonella* infection, leading to the formation of protrusions. The size of these protrusions is limited by villin-severing activities, enabling the formation of a structured network of actin filaments that constitute the ruffle. We showed that ruffle extremities consist mainly of villin accumulation. Similar dominant concentrations of villin on actin have been demonstrated at the leading edge of migrating cells (Nusrat et al., 1992; Ubelmann et al., 2013), suggesting an important role of villin in highly dynamic cellular processes. Thus, this villin layer could determine the limit of actin filaments extension. In absence of villin, the polymerization of filaments is not controlled, leading to the formation of abnormal extensions resembling giant microvilli, as observed by SEM. Interestingly, these aberrant ruffles are similar to those observed in nonpolarized cells such as HeLa cells, indicating that villin is a key factor in the invasion of differentiated cells. Moreover, our work indicates that villin recruitment to dynamic zones of bacterial entry sites to sever and depolymerize actin filaments can promote the creation of barbed ends to serve as new nuclei to further promote polymerization. In parallel, depolymerization enables the increase of the local pool of G-actin that becomes available for further polymerization. In the absence of a structured actin network, we could also hypothesize that membrane protein localization can be affected, such as cytoskeletal proteins that are supposed to interact with actin to promote bacterial internalization.

Villin regulatory activities have to be tightly controlled during infection to enable optimal invasion. In particular, severing activities of villin are obvious targets and potentially temporally and spatially regulated to permit ruffle resolution and membrane refolding following bacterial internalization. We demonstrated a mechanism through which membrane ruffling involves a time-dependent phosphorylation of villin. Changes in the phosphorylation status of villin are early and rapid events that are prone to complex regulations that allow efficient entry, but they also appear to be simultaneous at the scale of a single ruffle. We have shown that the kinase c-Src is responsible for transient villin phosphorylation during the infection. This phosphorylation occurs within minutes after the beginning of the invasion process. Villin phosphorylation is known to activate its severing activities and therefore may be important to promote organized membrane ruffling at the leading edge. However, a rapid dephosphorylation cascade induced by the bacterial factor SptP follows this phosphorylation wave. This certainly diminishes villin-severing capacities, thus enabling the reconstruction of microvilli after invasion of IECs. Moreover, the increase of phosphorylation observed with the SptP mutant does not persist, indicating that either other factors are involved in villin dephosphorylation

(C) Villin (red) and actin (green) distribution in sh-scr cells infected with WT *Salmonella* or *SipA* (gray) for 15 or 60 min. In the right lower panel, a magnification of ruffles induced by *SipA* shows the existence of characteristic protrusions at the cell periphery.

(D) Rhodamin-F-actin (2 μM) was polymerized and mixed with WT villin protein (Vill, 5 μM) or a mutated isoform (VillΔsev, 5 μM) in the presence or absence of SipA or the shorter isoforms $SipA^{514-657}$, $SipA^{514-640}$, or $SipA^{514-657,K635A\ E637W}$ (5 μM). Depolymerization was observed after 1 hr by confocal microscopy.

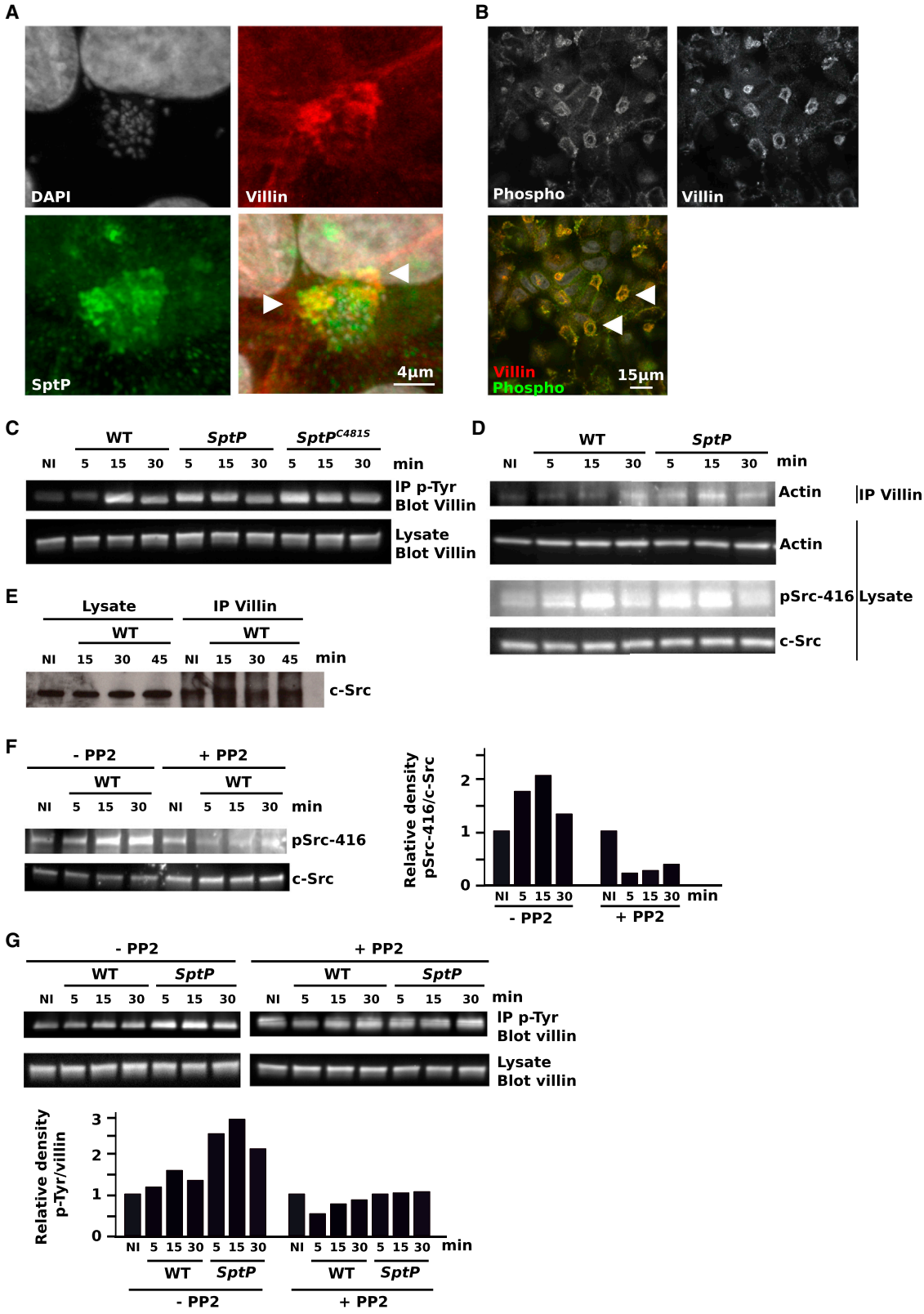

Figure 5. Villin Phosphorylation Is Regulated by SptP and c-Src

(A) Villin (red) and SptP (green) distribution in sh-scr cells infected with *Salmonella* for 60 min. Nuclei were counterstained with DAPI (gray). The white arrows indicate the sites of colocalization.

(legend continued on next page)

or villin phosphorylation is highly transient and does not persist over the time of infection.

We identified that villin phosphorylation regulates villin binding to actin. At first sight, this is not in agreement with published results that showed that villin phosphorylation decreases the binding activity of villin for F-actin in vitro (Zhai et al., 2001). However, in our experiment, we were not able to distinguish between F- and G-actin. As villin can bind both types of actin, we therefore cannot exclude that villin phosphorylation could favor the binding of one type of molecule over the other in infected cells to promote invasion. This modification in actin binding may be highly localized and participate in the construction of a precise but dynamic actin network. A decrease in actin binding is essential for the last steps of the entry process to inhibit the actin-modifying protein villin, thus enabling the resolution of apical membrane alterations. Moreover, altering villin phosphorylation could modify its ligand binding abilities and therefore modify its localization close to the membrane.

Our results indicate that SipA-bound F-actin is resistant to villin-induced depolymerization. Thus SipA inhibits actin depolymerization through villin in IECs. This inhibition may result in the accumulation of F-actin at the entry site to favor ruffle formation and bacterial entry. SipA may support actin assembly even though the free G-actin content is below the critical concentration that is physiologically necessary for actin polymerization. However, the G- and F-actin contents are not modified during infection. This indicates that, although villin-severing activities are locally inhibited by SipA to promote polymerization, villin is still active at the global cell level to renew the pool of free G-actin.

Villin activities are also regulated through calcium and ligand binding. It has been demonstrated that *Salmonella* entry induces intracellular calcium release (Ruschkowski et al., 1992), which is susceptible to activate villin-severing activities. Furthermore, it would be interesting to test how LPA and PIP2 binding could affect villin activities toward actin. Indeed, it has been shown that the association of villin with LPA inhibits its actin regulatory functions (Tomar et al., 2009), whereas association of villin with PIP2 inhibits actin depolymerization and enhances actin cross-linking by villin (Kumar et al., 2004b). The bacterial effector SopB is known to hydrolyze PIP2 to PI5P during *Salmonella* invasion (Mason et al., 2007). *Salmonella* ruffles are enriched in PIP2 in the outer region, but not in the invaginating region. In the absence of SopB, PIP2 is not hydrolyzed, and fission of the invaginating membranes is delayed due to stronger rigidity of the membrane (Terebiznik et al., 2002). We hypothesize that PIP2 can recruit and sequester villin in association with actin at the membrane during *Salmonella* infection and that the hydrolysis of PIP2 by SopB participates in membrane invagination by activating villin-severing activities and modifying actin structure.

Villin is not the only ABP with a severing activity expressed in the IECs. Other specific host ABPs may be redundant to promote ruffling and brush border reparation during bacterial invasion. The ABPs cofilin/ADF and gelsolin are also present in the IECs and are potential targets during *Salmonella* invasion. Cofilin and ADF depolymerizing activities play a major role in bacterial entry (Dai et al., 2004). In fact, these proteins are first dephosphorylated during infection by the host phosphatase Slingshot and then rephosphorylated by the host LIM kinase 1 in order to activate them. However, cofilin is not present in the brush border (Ashworth et al., 2004), and all experiments were performed in nonpolarized HeLa or Hek-293 cells (Dai et al., 2004). Similarly, gelsolin function during *Salmonella* entry has been studied in vitro, showing that it is primarily necessary for actin severing, and that its activity is inhibited by SipA, similar to villin inhibition. Nevertheless, gelsolin is expressed not in the microvilli of the brush border but in the terminal web, displaying a different pattern from that reported for villin. This emphasizes that, even if these ABPs are functionally similar to villin and are potentially recruited during bacterial invasion, they may have different impact on *Salmonella* entry due to their various locations and alternative regulations in the course of infection (Yin et al., 1981). They could only be involved in later steps of the invasion process, after the initiation of entry by the microvillus-resident villin. Consequently, in the context of the subversion of the brush border by *Salmonella*, villin appears as the primary target for the regulation of the actin cytoskeleton remodeling.

EXPERIMENTAL PROCEDURES

Cell Culture

TC7 cells, a subclone of Caco-2 cells, were maintained in DMEM 4.5 g/l of glucose (Life technologies) with 1% penicillin-streptomycin, 1% NEAA, and 20% heat-inactivated fetal bovine serum (FBS) at 37°C in 10% CO_2. Cells were seeded at 1×10^5 cells per well in 12-well tissue culture plates containing or not coverslips and maintained as differentiated monolayers for 21–28 days. For PP2 treatment (P0042, Sigma), cells are incubated 2 hr prior infection with the inhibitor (10 μM). PP2 treatment is maintained during the infection.

(B) Immunostaining of sh-scr cells infected for 60 min with *Salmonella* with anti-villin (red) and anti-phospho-tyrosine (green) antibodies. The white arrows indicate the sites of colocalization.

(C) sh-scr cells were infected with WT *Salmonella*, *SptP*, and $SptP^{C481S}$ (MOI 100) for the indicated time periods, and immunoprecipitation of phosphorylated proteins with an anti-phospho-tyrosine (p-Tyr) antibody was performed. Villin was detected by western blot in the immunoprecipitated fractions and in the total extracts.

(D) sh-scr cells were infected with WT *Salmonella* or *SptP* (MOI 100) for the indicated time periods, and immunoprecipitation of villin was performed. Actin was detected by western blot in the immunoprecipitated fractions and in the total extracts. pSrc-416 and c-Src were detected in the lysates.

(E) sh-scr cells were infected with *Salmonella* (MOI 100) and immunoprecipitation of villin was performed. c-Src was detected by western blot in the immunoprecipitated fractions and in the total extracts.

(F) Representative pSrc-416 and c-Src detection by western blot on total lysates from sh-scr cells infected with *Salmonella* in presence or not of PP2. Densitometric ratio is presented in the graph.

(G) sh-scr cells were infected with WT *Salmonella* or *SptP* (MOI 100) for the indicated time periods and immunoprecipitation of tyrosine-phosphorylated proteins was performed in presence or not of PP2. Villin was detected by western blot in the immunoprecipitated fractions and in the total extracts. Densitometric ratio is presented in the graph.

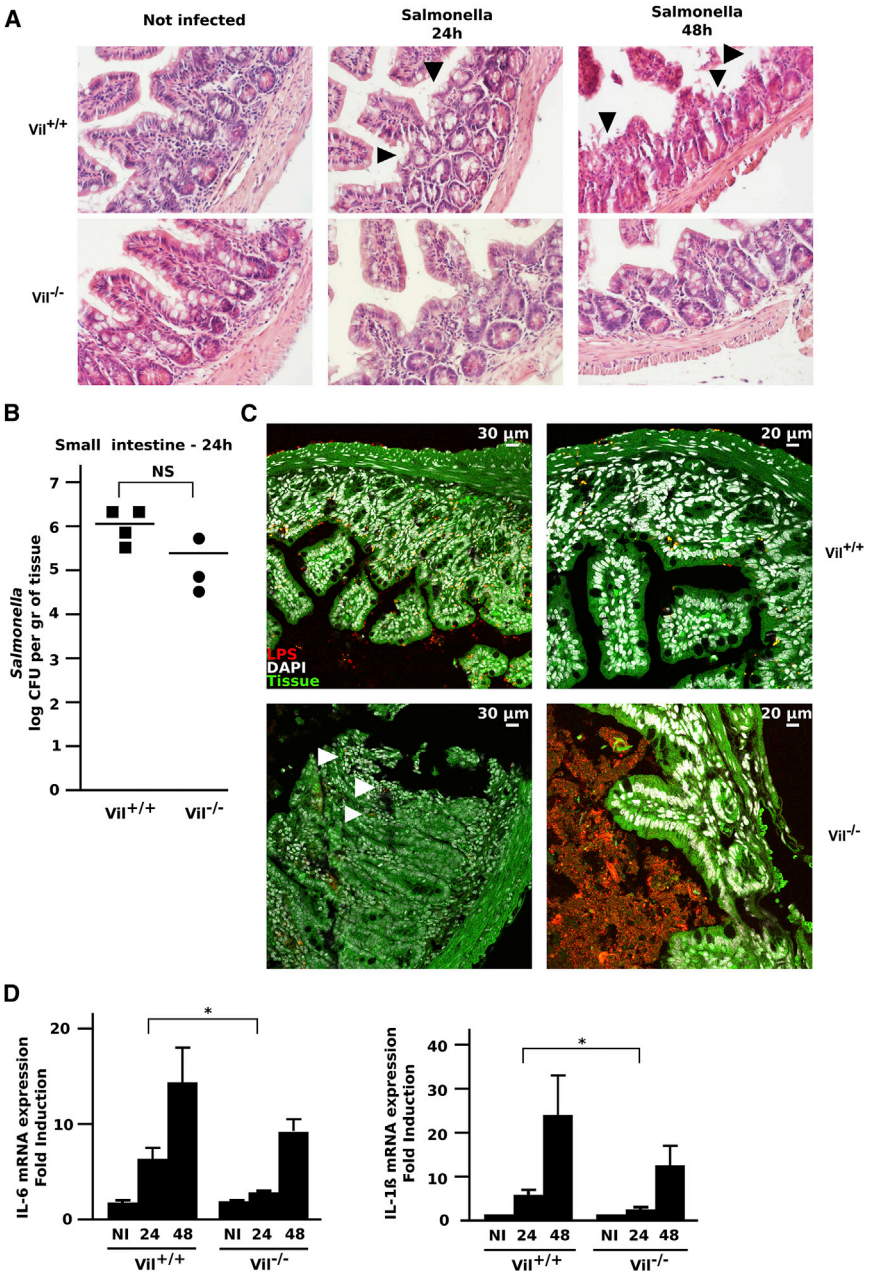

Figure 6. Villin Knockout Mice Are More Resistant to *Salmonella* Infection

(A) H&E-stained distal ileal sections from *Vil*$^{+/+}$ or *Vil*$^{-/-}$ mice infected with *Salmonella*. *Vil*$^{-/-}$ samples display a stronger inflammation and destruction after *Salmonella* infection at 24 and 48 hr p.i. (black arrowheads). Magnification: 40×.

(B) Bacterial colonization in the small intestine 24h p.i. with *Salmonella*. Significance determined with the Mann-Whitney U test and expressed as the median (NS, not significant).

(C) Intracellular *Salmonella* from *Vil*$^{+/+}$ or *Vil*$^{-/-}$ mice were identified by anti-LPS staining (red) in distal ileal sections at 72 hr p.i. Nuclei are counterstained with DAPI (white); the intestinal tissue is seen in green (autofluorescence). Two areas are shown for each genotype. White arrowheads indicate sites of invasion.

(D) Gene expression quantification by RT-qPCR. *IL-6* and *IL-1β* expression was measured in noninfected mice (NI) and at 24 or 48 hr p.i. Data are represented as mean ± SEM (*p < 0.05).

Bacterial Strains and Culture Conditions

Bacteria were cultured O/N at 37°C with shaking in Luria Broth medium, pelleted at 5,000 × *g* for 5 min, washed in PBS, and resuspended in DMEM complemented with HEPES 50 mM. The inoculum was diluted to the requested MOI and added to the cells at 37°C. *S. typhimurium* strains were isogenic derivatives of the naturally streptomycin-resistant WT strain *SL1344* (Hoiseth and Stocker, 1981). The strains *SL1344 ΔSipA*, *ΔSipC*, *ΔSptP*, and *ΔSopE-SopE2-SopB-SipA* (called *Δ4* in this study) were also used (Hapfelmeier and Hardt, 2005) as well as the WT strain *SB300* and the isogenic mutants *ΔSptP and SptP*^{C481S} (Murli et al., 2001).

Cell Infection and Immunofluorescence Microscopy

Differentiated cells were washed with DMEM, and *Salmonella* were added directly to the cells (MOI 20). After infection, cells were fixed with PFA 3.8% for 15 min at RT and washed with PBS. Cells were permeabilized for 20 min in 0.1% Triton X-100, and saturation was performed with 3% BSA, 5% FBS in PBS for 30 min. The coverslips were then incubated with the appropriate primary antibody for 1 hr at RT. The coverslips were washed in PBS, incubated with the secondary antibody for 1 hr, washed again in PBS, and incubated with DAPI for 2 min. Coverslips were mounted onto glass slides with ProLong Gold antifade reagent (Life Technologies). Images were collected using a confocal microscope with a 60×, 1.4 NA oil immersion objective (SP5 Leica). Images comparing different genotypes or experimental conditions were acquired and postprocessed with identical parameters. All images were processed and pseudocolored using ImageJ (National Institutes of Health) or Imaris software.

Mice Infection

Wild-type (*Vil*$^{+/+}$) and isogenic villin knockout mice (*Vil*$^{-/-}$) (Ferrary et al., 1999) were bred in a C57BL/6J background. *tgvillinWT* and *tgvillinΔsev* mice were obtained after tamoxifen treatment as previously described (Ubelmann et al., 2013). Briefly, mice, including controls, were injected intraperitoneally with tamoxifen (50 µg/g of animal body weight) on two consecutive days/week for a total of 4 weeks. All mice were kept in a specific pathogen-free area. For bacterial infection, streptomycin-pretreated mice (20 mg/animal) were infected by gavage with O/N cultures of *Salmonella SL1344* (5 × 10^7 bacteria in 100 µl). Bacterial colonization was determined by plating. Briefly, mice were euthanized, and tissue samples were removed for bacterial quantification and weighted. Samples were homogenized using a Precellys homogenizer (Ozyme) for 2 × 15 s at a frequency of 5,000 rpm. Samples were diluted in PBS and plated for colony counts. Each experiment was repeated three times with a minimum of three animals per group. All animal experiments were carried out under approval by the Use Committee of Pasteur Institute and by the French Ministry of Agriculture (Ethic committee protocol number: 2013-0028).

Statistical Analysis

Statistical analysis was conducted using the software GraphPad Prism (v5.0). The mean ± SEM from at least three independent experiments is shown in figures. p values were calculated using Mann-Whitney or unpaired t tests.

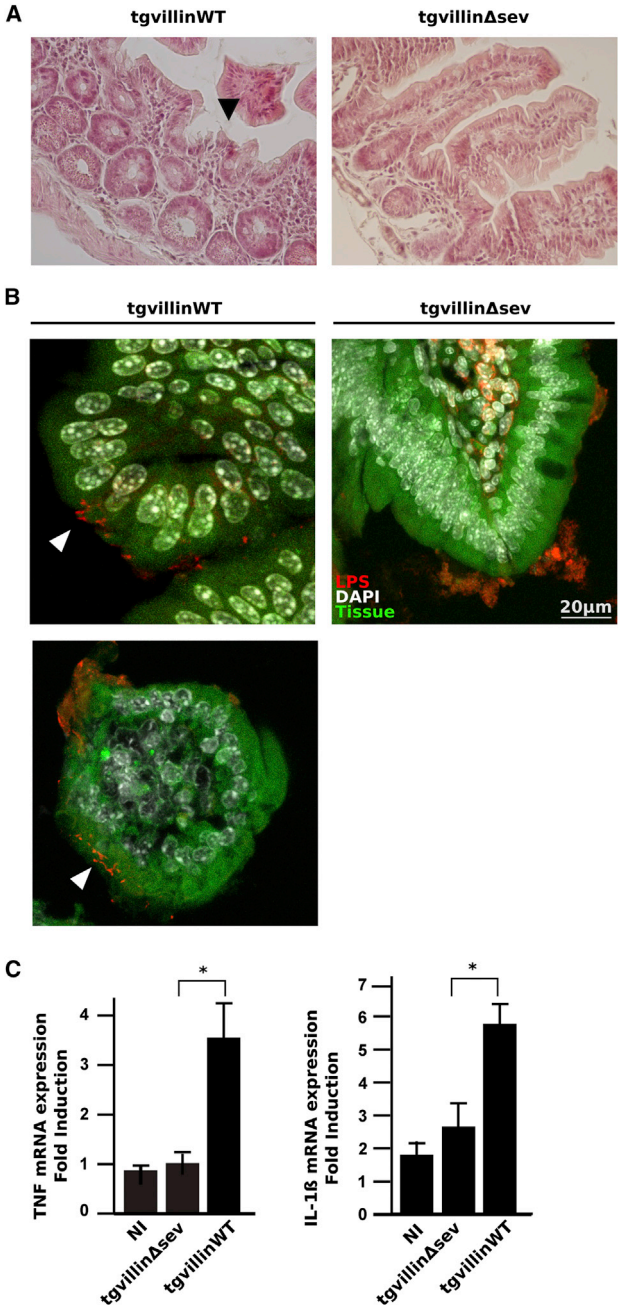

Figure 7. The Severing Activity of Villin Is Required for *Salmonella* Infection In Vivo

(A) H&E-stained distal ileal sections from *tgvillinWT* or *tgvillinΔsev* mice infected with *Salmonella* for 24 hr. Epithelial destruction in *tgvillinWT* mice is more important compared to *tgvillinΔsev* after infection (Black arrow). Magnification: 40×.

(B) Intracellular *Salmonella* from *tgvillinWT* or *tgvillinΔsev* mice were identified by anti-LPS staining (red) in distal ileal sections at 24 hr p.i. Nuclei are counterstained with DAPI (white), and the intestinal tissue is seen in green (autofluorescence). Entry sites are indicated with white arrowheads. Upper part: longitudinal section of a villus; lower part: transversal section of a villus.

(C) Gene expression quantification by RT-qPCR. *TNF* and *IL-1β* expressions were measured in noninfected mice (NI) and 24 hr p.i. with *Salmonella* in *tgvillinWT* and *tgvillinΔsev* mice. Data are represented as mean ± SEM (*$p < 0.05$, Mann-Whitney).

SUPPLEMENTAL INFORMATION

Supplemental Information includes one figure and Supplemental Experimental Procedures and can be found with this article online at http://dx.doi.org/10.1016/j.chom.2014.12.003.

ACKNOWLEDGMENTS

We thank R. Friedman, C. Mulet and T. Pedron for technical help. We thank T. Marlovits for antibodies, H.D. Hardt and J. Galan for *Salmonella* strains, and D. Zhou and V. Koronakis for plasmids. We acknowledge France-BioImaging infrastructure supported by the French National Research Agency (ANR-10-INSB-04-01, «Investments for the future»). This work was supported by the ERC (P.S. Advanced Grant HOMEOEPITH, number 232798). P.J.S. is an HHMI senior foreign scholar. The authors declare no conflict of interest.

Received: April 8, 2014
Revised: September 16, 2014
Accepted: December 4, 2014
Published: January 15, 2015

REFERENCES

Agbor, T.A., and McCormick, B.A. (2011). Salmonella effectors: important players modulating host cell function during infection. Cell. Microbiol. *13*, 1858–1869.

Ashworth, S.L., Wean, S.E., Campos, S.B., Temm-Grove, C.J., Southgate, E.L., Vrhovski, B., Gunning, P., Weinberger, R.P., and Molitoris, B.A. (2004). Renal ischemia induces tropomyosin dissociation-destabilizing microvilli microfilaments. Am. J. Physiol. Renal Physiol. *286*, F988–F996.

Athman, R., Fernandez, M.I., Gounon, P., Sansonetti, P., Louvard, D., Philpott, D., and Robine, S. (2005). Shigella flexneri infection is dependent on villin in the mouse intestine and in primary cultures of intestinal epithelial cells. Cell. Microbiol. *7*, 1109–1116.

Bretscher, A., and Weber, K. (1980). Villin is a major protein of the microvillus cytoskeleton which binds both G and F actin in a calcium-dependent manner. Cell *20*, 839–847.

Dai, S., Sarmiere, P.D., Wiggan, O., Bamburg, J.R., and Zhou, D. (2004). Efficient Salmonella entry requires activity cycles of host ADF and cofilin. Cell. Microbiol. *6*, 459–471.

Fernandez, M.I., Thuizat, A., Pedron, T., Neutra, M., Phalipon, A., and Sansonetti, P.J. (2003). A newborn mouse model for the study of intestinal pathogenesis of shigellosis. Cell. Microbiol. *5*, 481–491.

Ferrary, E., Cohen-Tannoudji, M., Pehau-Arnaudet, G., Lapillonne, A., Athman, R., Ruiz, T., Boulouha, L., El Marjou, F., Doye, A., Fontaine, J.J., et al. (1999). In vivo, villin is required for Ca(2+)-dependent F-actin disruption in intestinal brush borders. J. Cell Biol. *146*, 819–830.

Finlay, B.B., and Falkow, S. (1990). Salmonella interactions with polarized human intestinal Caco-2 epithelial cells. J. Infect. Dis. *162*, 1096–1106.

Forney, J.R., DeWald, D.B., Yang, S., Speer, C.A., and Healey, M.C. (1999). A role for host phosphoinositide 3-kinase and cytoskeletal remodeling during Cryptosporidium parvum infection. Infect. Immun. *67*, 844–852.

Friederich, E., Huet, C., Arpin, M., and Louvard, D. (1989). Villin induces microvilli growth and actin redistribution in transfected fibroblasts. Cell *59*, 461–475.

Fu, Y., and Galán, J.E. (1999). A salmonella protein antagonizes Rac-1 and Cdc42 to mediate host-cell recovery after bacterial invasion. Nature *401*, 293–297.

Hapfelmeier, S., and Hardt, W.D. (2005). A mouse model for S. typhimurium-induced enterocolitis. Trends Microbiol. *13*, 497–503.

Hardt, W.D., Chen, L.M., Schuebel, K.E., Bustelo, X.R., and Galán, J.E. (1998). S. typhimurium encodes an activator of Rho GTPases that induces membrane ruffling and nuclear responses in host cells. Cell *93*, 815–826.

Hayward, R.D., and Koronakis, V. (1999). Direct nucleation and bundling of actin by the SipC protein of invasive Salmonella. EMBO J. *18*, 4926–4934.

Higashide, W., Dai, S., Hombs, V.P., and Zhou, D. (2002). Involvement of SipA in modulating actin dynamics during Salmonella invasion into cultured epithelial cells. Cell. Microbiol. *4*, 357–365.

Hoiseth, S.K., and Stocker, B.A. (1981). Aromatic-dependent Salmonella typhimurium are non-virulent and effective as live vaccines. Nature *291*, 238–239.

Hong, K.H., and Miller, V.L. (1998). Identification of a novel Salmonella invasion locus homologous to Shigella ipgDE. J. Bacteriol. *180*, 1793–1802.

Khurana, S., and George, S.P. (2008). Regulation of cell structure and function by actin-binding proteins: villin's perspective. FEBS Lett. *582*, 2128–2139.

Kumar, N., and Khurana, S. (2004). Identification of a functional switch for actin severing by cytoskeletal proteins. J. Biol. Chem. *279*, 24915–24918.

Kumar, N., Tomar, A., Parrill, A.L., and Khurana, S. (2004a). Functional dissection and molecular characterization of calcium-sensitive actin-capping and actin-depolymerizing sites in villin. J. Biol. Chem. *279*, 45036–45046.

Kumar, N., Zhao, P., Tomar, A., Galea, C.A., and Khurana, S. (2004b). Association of villin with phosphatidylinositol 4,5-bisphosphate regulates the actin cytoskeleton. J. Biol. Chem. *279*, 3096–3110.

Lauwaet, T., Oliveira, M.J., Callewaert, B., De Bruyne, G., Saelens, X., Ankri, S., Vandenabeele, P., Mirelman, D., Mareel, M., and Leroy, A. (2003). Proteolysis of enteric cell villin by Entamoeba histolytica cysteine proteinases. J. Biol. Chem. *278*, 22650–22656.

Li, D., Wang, X., Wang, L., and Zhou, D. (2013). The actin-polymerizing activity of SipA is not essential for Salmonella enterica serovar Typhimurium-induced mucosal inflammation. Infect. Immun. *81*, 1541–1549.

Lorkowski, M., Felipe-López, A., Danzer, C.A., Hansmeier, N., and Hensel, M. (2014). Salmonella enterica invasion of polarized epithelial cells is a highly cooperative effort. Infect. Immun. *82*, 2657–2667.

Ly, K.T., and Casanova, J.E. (2007). Mechanisms of Salmonella entry into host cells. Cell. Microbiol. *9*, 2103–2111.

Mason, D., Mallo, G.V., Terebiznik, M.R., Payrastre, B., Finlay, B.B., Brumell, J.H., Rameh, L., and Grinstein, S. (2007). Alteration of epithelial structure and function associated with PtdIns(4,5)P2 degradation by a bacterial phosphatase. J. Gen. Physiol. *129*, 267–283.

Mathew, S., George, S.P., Wang, Y., Siddiqui, M.R., Srinivasan, K., Tan, L., and Khurana, S. (2008). Potential molecular mechanism for c-Src kinase-mediated regulation of intestinal cell migration. J. Biol. Chem. *283*, 22709–22722.

McGhie, E.J., Hayward, R.D., and Koronakis, V. (2001). Cooperation between actin-binding proteins of invasive Salmonella: SipA potentiates SipC nucleation and bundling of actin. EMBO J. *20*, 2131–2139.

McGhie, E.J., Hayward, R.D., and Koronakis, V. (2004). Control of actin turnover by a salmonella invasion protein. Mol. Cell *13*, 497–510.

Mogilner, A., and Rubinstein, B. (2005). The physics of filopodial protrusion. Biophys. J. *89*, 782–795.

Murli, S., Watson, R.O., and Galán, J.E. (2001). Role of tyrosine kinases and the tyrosine phosphatase SptP in the interaction of Salmonella with host cells. Cell. Microbiol. *3*, 795–810.

Nusrat, A., Delp, C., and Madara, J.L. (1992). Intestinal epithelial restitution. Characterization of a cell culture model and mapping of cytoskeletal elements in migrating cells. J. Clin. Invest. *89*, 1501–1511.

Revenu, C., Courtois, M., Michelot, A., Sykes, C., Louvard, D., and Robine, S. (2007). Villin severing activity enhances actin-based motility in vivo. Mol. Biol. Cell *18*, 827–838.

Revenu, C., Ubelmann, F., Hurbain, I., El-Marjou, F., Dingli, F., Loew, D., Delacour, D., Gilet, J., Brot-Laroche, E., Rivero, F., et al. (2012). A new role for the architecture of microvillar actin bundles in apical retention of membrane proteins. Mol. Biol. Cell *23*, 324–336.

Ruschkowski, S., Rosenshine, I., and Finlay, B.B. (1992). Salmonella typhimurium induces an inositol phosphate flux in infected epithelial cells. FEMS Microbiol. Lett. *74*, 121–126.

Steele-Mortimer, O., Knodler, L.A., Marcus, S.L., Scheid, M.P., Goh, B., Pfeifer, C.G., Duronio, V., and Finlay, B.B. (2000). Activation of Akt/protein kinase B in epithelial cells by the Salmonella typhimurium effector sigD. J. Biol. Chem. *275*, 37718–37724.

Stender, S., Friebel, A., Linder, S., Rohde, M., Mirold, S., and Hardt, W.D. (2000). Identification of SopE2 from Salmonella typhimurium, a conserved guanine nucleotide exchange factor for Cdc42 of the host cell. Mol. Microbiol. *36*, 1206–1221.

Temm-Grove, C.J., Jockusch, B.M., Rohde, M., Niebuhr, K., Chakraborty, T., and Wehland, J. (1994). Exploitation of microfilament proteins by Listeria monocytogenes: microvillus-like composition of the comet tails and vectorial spreading in polarized epithelial sheets. J. Cell Sci. *107*, 2951–2960.

Terebiznik, M.R., Vieira, O.V., Marcus, S.L., Slade, A., Yip, C.M., Trimble, W.S., Meyer, T., Finlay, B.B., and Grinstein, S. (2002). Elimination of host cell PtdIns(4,5)P(2) by bacterial SigD promotes membrane fission during invasion by Salmonella. Nat. Cell Biol. *4*, 766–773.

Tomar, A., Wang, Y., Kumar, N., George, S., Ceacareanu, B., Hassid, A., Chapman, K.E., Aryal, A.M., Waters, C.M., and Khurana, S. (2004). Regulation of cell motility by tyrosine phosphorylated villin. Mol. Biol. Cell *15*, 4807–4817.

Tomar, A., George, S.P., Mathew, S., and Khurana, S. (2009). Differential effects of lysophosphatidic acid and phosphatidylinositol 4,5-bisphosphate on actin dynamics by direct association with the actin-binding protein villin. J. Biol. Chem. *284*, 35278–35282.

Ubelmann, F., Chamaillard, M., El-Marjou, F., Simon, A., Netter, J., Vignjevic, D., Nichols, B.L., Quezada-Calvillo, R., Grandjean, T., Louvard, D., et al. (2013). Enterocyte loss of polarity and gut wound healing rely upon the F-actin-severing function of villin. Proc. Natl. Acad. Sci. USA *110*, E1380–E1389.

Wang, Y., George, S.P., Srinivasan, K., Patnaik, S., and Khurana, S. (2012). Actin reorganization as the molecular basis for the regulation of apoptosis in gastrointestinal epithelial cells. Cell Death Differ. *19*, 1514–1524.

Watson, K.G., and Holden, D.W. (2010). Dynamics of growth and dissemination of Salmonella in vivo. Cell. Microbiol. *12*, 1389–1397.

Wells, C.L., van de Westerlo, E.M., Jechorek, R.P., Haines, H.M., and Erlandsen, S.L. (1998). Cytochalasin-induced actin disruption of polarized enterocytes can augment internalization of bacteria. Infect. Immun. *66*, 2410–2419.

Yin, H.L., Albrecht, J.H., and Fattoum, A. (1981). Identification of gelsolin, a Ca2+-dependent regulatory protein of actin gel-sol transformation, and its intracellular distribution in a variety of cells and tissues. J. Cell Biol. *91*, 901–906.

Zhai, L., et al. (2001). Tyrosine phosphorylation of villin regulates the organization of the actin cytoskeleton. J. Biol. Chem. *27*, 36163–36167.

Zhou, D., Mooseker, M.S., and Galán, J.E. (1999a). An invasion-associated Salmonella protein modulates the actin-bundling activity of plastin. Proc. Natl. Acad. Sci. USA *96*, 10176–10181.

Zhou, D., Mooseker, M.S., and Galán, J.E. (1999b). Role of the S. typhimurium actin-binding protein SipA in bacterial internalization. Science *283*, 2092–2095.

Zhou, D., Chen, L.M., Hernandez, L., Shears, S.B., and Galán, J.E. (2001). A Salmonella inositol polyphosphatase acts in conjunction with other bacterial effectors to promote host cell actin cytoskeleton rearrangements and bacterial internalization. Mol. Microbiol. *39*, 248–259.